Phase Composition of Block Copoly(ether ester) Thermoplastic Elastomers Studied by Solid-State NMR Techniques

V. M. Litvinov,*,† M. Bertmer,‡ L. Gasper,‡ D. E. Demco,‡ and B. Blümich‡

DSM Research, P.O. Box 18, 6160MD, Geleen, The Netherlands, and Institute for Technical Chemistry and Macromolecular Chemistry, RWTH Aachen, Worringer Weg 1, 52056 Aachen, Germany

Received June 9, 2003

ABSTRACT: The microphase composition of poly(butylene terephthalate)-*block*-poly(tetramethylene oxide) multiblock (PBT-*block*-PTMO) copolymers with varying content of PTMO soft block and varying block length was studied by ^{1}H NMR transverse magnetization relaxation (T_2 relaxation) and ^{1}H 2D DQ NMR experiments under fast MAS. The 2D NMR method showed the existence of the molecular scale mixing of PBT and PTMO blocks. The ^{1}H and previously obtained ^{13}C NMR relaxation data provided detailed information on the microphase composition. The content of soft domains (i.e., viscoelastic material which is composed of the soft block and mixed PBT) and hard domains (i.e., crystalline PBT and immobilized PBT chain portions at the crystal−amorphous PBT interface) depends largely on temperature. It was shown that about 15−25% of PBT in the samples is soft due to molecular mixing with PTMO. The results suggest that at 40 °C the mixed phase is composed of approximately one PBT chain unit per eight PTMO chain units. The PBT crystallinity in the copolymers slightly increases with increasing length of the soft block, since this causes increase of the average length of PBT blocks. The content of crystalline PBT is nearly constant for samples with hard blocks containing more than five monomer units and decreases for shorter PBT block lengths. An increase in the content of PTMO with the same block length causes a significant increase in chain mobility in the soft domains. Apparently, the content of the mixed phase and the density of physical/topological junctions at the PBT/PTMO interphase largely affect the molecular mobility in the soft domains.

Introduction

Thermoplastic elastomers (TPE) are industrially important polymers due to a combination of the elastic properties of rubber with the processability of thermoplastic polymers.[1] Since TPE can be processed from the melt, this enables product design not easily achievable for conventional rubber. Multiblock copolymers consisting of elastic and rigid blocks, which are immiscible or partly miscible, belong to the class of TPEs. The phase separation causes formation of rigid and soft domains providing material with a good combination of elasticity and mechanical strength. Rigid domains, which are interconnected by elastic chains of elastic blocks, act as multifunctional physical network junctions responsible for the elasticity of the material. The structure of this physical network is largely determined by the size, shape, and dispersion of the rigid domains, which are largely affected by the composition and the length of the elastic and rigid blocks. Therefore, knowledge of the microphase structure of TPEs is of great importance for a good understanding of their macroscopic properties.

The segmented block copoly(ether esters) are one of the most extensively studied TPEs.[1] Block copolymers of poly(butylene terephthalate) (PBT) and poly(tetramethylene oxide) (PTMO), PBT-*block*-PTMO, are of special interest since they combine good low-temperature flexibility with excellent mechanical properties and thermooxidative stability up to high temperatures as well as a good resistance against many chemicals. Since PBT has a high melting temperature and PTMO a low T_g, this TPE possesses a wide temperature range for applications. The mechanical properties of PBT-*block*-PTMO are largely affected by (1) the phase structure, i.e., the crystallinity of PBT and PTMO, the crystal size and perfection, and the fraction of the mixed PBT/PTMO phase and (2) the morphology, i.e., continuity of the different phases (i.e., disperse vs co-continuous), and the size and shape of soft and hard domains.

The phase structure and morphology of PBT-*block*-PTMO were studied by several authors using various techniques. The results of these studies have recently been summarized.[2] Usually, the copoly(ether ester) with a relatively short block length forms a homogeneous mixture in the molten state. Several authors have shown that PBT crystallization is the driving force for phase separation causing the formation of a co-continuous two-phase morphology.[3−6] Upon crystallization, PBT forms well-developed spherolithic structures with diameters of about 5−20 μm.[2] The domain sizes of the amorphous phase seem to increase with concentration and block length of the soft blocks and range between 10 and 30 nm.[2]

The phase transitions in PBT-*block*-PTMO were studied by differential scanning calorimetry (DSC).[2,6,7] The melting temperature of PTMO and PBT crystals in PBT-*block*-PTMO is significantly lower than that of the pure homopolymers, i.e., −20 to 0 °C or not detectable for PTMO in TPE against about 35 °C for pure PTMO, and 157−225 °C for PBT in PBT-*block*-PTMO against about 230 °C for pure PBT.[2,7] The decrease in melting temperature in the copolymers is apparently caused by smaller crystal sizes, as compared to that for the homopolymers, and crystal imperfections due to short block length and mutual constraints from both blocks on PTMO and PBT crystallization. The ability of PTMO blocks to crystallize suggests the presence of a PTMO-rich phase. The first glass transition at about

† DSM Research.
‡ Institute for Technical Chemistry and Macromolecular Chemistry.
* To whom correspondence should be addressed.

10.1021/ma030314h CCC: $25.00
Published on Web 09/12/2003

−70 to −60 °C was assigned to the amorphous PTMO blocks in PBT-*block*-PTMO.[2,6,7] Since this temperature is higher than that of pure PTMO (−90 °C), this suggests largely constrained chain mobility of the soft block due to its chemical linkage to the hard block and possibly partial mixing of PTMO with PBT. The second glass transition in the range of −50 to −20 °C was assigned to a mixed PBT/PTMO amorphous phase.[7] The third DSC endo peak in the range 30−50 °C may be attributed to structural reorganizations of the hard blocks.[7] DSC experiments do not detect glass transition of amorphous PBT in PBT-*block*-PTMO,[7] which might suggest that noncrystallizable PBT chain units are mixed with PTMO.

The crystallinity of PBT and PTMO blocks and the structural rearrangement under uniaxial stretching were studied with stretching DSC, WAXD, SAXS,[7] and ^{13}C NMR.[8] The crystallinity increases with increasing PBT block content and the length of the PTMO block, since these changes in the structure of PBT-*block*-PTMO cause an increase in PBT block length. The WAXD degree of PBT crystallinity, which is normalized to the PBT content, varies from 15 to 30%. Samples with higher crystallinity have a more perfect crystalline structure and larger lateral crystallite size, which is in the range 16.5−20 nm.[7] The supramolecular structure of PBT-*block*-PTMO was studied with X-rays.[7] According to WAXD data,[7] only PBT fragments with the number-average degree of polymerization longer than eight butylene terephthalate units can form crystallites. Therefore, the molar mass of the PBT blocks affects not only the number and the sizes of the PBT crystallites but also the content of PBT fragments in the amorphous phase. It is noted that the length of the PBT block increases with increasing PBT content and increasing PTMO block length. Stretching of PBT-*block*-PTMO with relatively long PTMO block length and high PTMO content causes strain-induced crystallization of PTMO.[8] The amount of crystalline PTMO increases linearly with the sample strain. Heating to 50 °C causes the strain-induced PTMO crystals to melt.

The miscibility of PBT and PTMO in the amorphous phase of PBT-*block*-PTMO was studied by solid-state NMR,[2,8] dynamic mechanical thermal analysis (DMTA),[2] and dielectric spectroscopy (DIES).[2] Microphase separation of the amorphous phase into a highly mobile PTMO-rich phase and a less mobile PBT/PTMO mixed phase or PBT/PTMO interface has been suggested by these studies. DMTA and DIES reveal two glass transitions, which could be assigned to two distinct amorphous phases with different chain mobility. The microphase separation is most pronounced in samples with long PTMO blocks and high PTMO content. Solid-state ^{13}C NMR relaxation experiments unambiguously show the presence of two types of PTMO chain units with distinctly different local chain mobility.[2,8] It was suggested in these studies that PTMO chain mobility in the homogeneously mixed PBT/PTMO phase is restricted by the presence of PBT segments due to coupling of chain motions of both blocks. However, motional heterogeneity of PTMO blocks can also be caused by a dynamical interface due to anchoring of soft blocks at rigid PBT domains, which can cause the apparent "two-phase" behavior.[9,10] It should be noted that the fraction of PTMO chain units that are adjacent to PBT blocks is rather large due to a relatively short PTMO block length, which varies in previously studied samples from about 14 to 28 elementary chain units.[2,7,8] The presence of a dynamic interface has been shown for a variety of polymeric materials,[11,12] such as block copolymers,[13] fillers with grafted chains,[14] ionomers,[15] filled rubbers,[16] and semicrystalline polymers.[17]

Table 1. Amount and Length of the Soft Block in (PBT-*block*-PTMO) Copolymers

	amount of PTMO block, wt %		
length of PTMO block, g/mol	35	50	60
1000	A1000/35	A1000/50	A1000/60
1500		A1500/50	A1500/60
2000			A2000/60

Table 2. PBT Crystallinity Measured by DSC[18] and the Number-Average Length of the PBT Blocks in (PBT-*block*-PTMO) Copolymers[a]

TPE-A series	PBT block length, butylenes terephthalate units	deg of crystallinity per total sample weight, %	fraction of crystalline PBT, %
A1000/35	9	30−34	47−52
A1000/50	5	21−22	41−45
A1500/50	7.5	21−22	43−46
A1000/60	3.5	12−13	30−32
A1500/60	5	16−17	40−44
A2000/60	6.5	16−17	39−43

[a] The molar mass distribution of the PBT blocks $M_w/M_n \approx 2$.

The aim of the present study is to determine the molecular origin of the PBT/PTMO mixed phase or interface and to obtain quantitative information about the phase composition of PBT-*block*-PTMO over a wide compositional range. These materials are analyzed with (1) proton NMR transverse magnetization relaxation that is used to determine the phase composition and molecular mobility in different phases and (2) a two-dimensional ^{1}H DQ BABA NMR experiment, which allows to study the molecular scale miscibility of PBT and PTMO blocks looking for correlation peaks between signals from the hard and soft blocks. The results of the present study are compared with previous investigations of the same materials with solid state ^{13}C NMR,[2,8] DSC,[2,7,18] and WAXD.[7]

Experimental Section

A. Sample Preparation and Characterization. The PBT/PTMO copoly(ether esters) were synthesized by melt transesterification and subsequent polycondensation of dimethyl terephthalate, 1,4-butanediol, and poly(tetrahydrofuran) with varying molecular weight, as described previously.[2] All samples were stabilized with 0.25 wt % Irganox 1330. The samples were injection-molded into test plates. All samples were cut out of the plates.

Two series of samples were studied. In the first series both the content of the soft block and its length were varied. Sample composition, block length, and sample designations for this series are given in Table 1. The average PBT block length decreases with increasing molar mass and weight fraction of the PTMO blocks (see Table 2). The PBT crystallinity, as measured by DSC,[18] and the mean length of the PBT blocks, which was calculated from the sample composition and PTMO block length, are given in Table 2. In the second series of samples, the molar mass of the soft block was 1000 g/mol, and the PTMO block content was varied from 10 to 60 wt % (Table 3). The content of the soft block was determined by accurate weighing of the ingredients for the synthesis and was confirmed by liquid-state ^{1}H NMR experiments at 383 K for samples dissolved in $C_2D_2Cl_4$. It is noted that $O(CH_2)_4$ fragments at the transition of the polyester to the polyether were counted as soft blocks, and all terephthalic units are counted as hard blocks.

Table 3. Composition of (PBT-*block*-PTMO) Copolymers and Fraction of Hydrogen in the Soft and Hard Blocks

TPE-B series	PTMO, wt %[a]	PTMO, wt %[b]	% H in PTMO[c]
B1000/10	10.0	10.0	25.35
B1000/25	25.0	25.6	50.46
B1000/30	30.0	29.5	62.20
B1000/35	35.0	35.1	62.20
B1000/48	48.0	47.9	73.82
B1000/50	50.0	49.4	74.34
B1000/60	60.0	59.7	82.09

[a] According to synthesis. [b] According to liquid-state NMR. [c] Calculated from sample composition according to synthesis.

A selectively deuterated PBT homopolymer was synthesized using 2,2,3,3-d_4-butylene glycol as the starting material, as described previously.[19]

B. **Equipment. 1. Proton NMR transverse magnetization relaxation decays** (T_2 relaxation decays) were measured on a Bruker Minispec NMS-120 spectrometer at a proton resonance frequency of 20 MHz. The duration of the 90° pulse and the dead time were 2.8 μs and 7 μs, respectively. This spectrometer was equipped with a BVT-3000 variable temperature unit.

NMR experiments as a function of temperature were performed by heating the samples from room temperature. The measurements at each temperature took about 1−1.5 h. No additional experiments were performed to study annealing of samples during experiments at elevated temperatures.

2. ^{1}H 2D DQ BABA experiments under fast MAS were performed on a Bruker DSX 500 spectrometer, operating at a proton frequency of 500.46 MHz using a 2.5 mm rotor at a spinning speed of 20 kHz. The 90° pulse length was 2 μs.

C. NMR Experiments and Data Analysis. 1. ^{1}H T_2 Relaxation Experiments. A solid echo pulse sequence (SEPS), $90°_x-t_{se}-90°_y-t_{se}-$[acquisition of the amplitude of the transverse magnetization $A(t)$], with $t_{se} = 10$ μs was used to measure the free induction decay (FID). The point in time from the beginning of the first pulse $t = 2t_{se} + t_{90}/2$ was taken as zero,[20] where t_{90} is the duration of the 90° pulse. The FID for PBT-*block*-PTMO consisted of two distinct components, as it will be shown below. The characteristic decay time of these components is typical for the relaxation of rigid (T_2^s relaxation) and soft (T_2^l relaxation) materials. It should be noted that the rigid/soft ratio measured with the SEPS can be somewhat lower than its actual value because of (i) the incomplete refocusing of the dipolar interaction by the solid echo for a dipolar network (see for instance ref 21), (ii) molecular motions, the correlation time of which is comparable to the pulse spacing,[22] and (iii) the shift of the echo maximum due to nonzero pulse width.[20,23] To estimate this systematic error, the SEPS experiment was performed at different t_{se} for the PBT homopolymer. It can be seen from Figure 1A that the initial amplitude of the fast [$A(0)^s$] and slowly [$A(0)^l$] decaying components decreases with increasing t_{se}. Because of faster decay of $A(0)$ for the rigid phase, the fraction of this phase appears about a few percent lower compared to its true value, as can be seen in Figure 1B.

A Hahn echo pulse sequence (HEPS), $90°_x-t_{He}-180°_x-t_{He}-$[acquisition $A(t)$ of the amplitude of an echo maximum], was used to record the slow part of the T_2 relaxation decay for the soft domains of the samples, where t_{He} was varied between 35 μs and 400 ms. The second pulse in the HEPS reverses the nuclear spin evolution of the mobile molecules only, and an echo signal is formed with a maximum at time $t = [2t_{He} + (t_{90}/2 + t_{180}/2)]$ from the beginning of the first pulse, where $t_{90}/2$ and $t_{180}/2$ are the half-time of the 90° and 180° pulse, respectively. By varying the pulse spacing in the HEPS, the amplitude of the transverse magnetization $A(t)$ is measured as a function of time t. The HEPS makes it possible to eliminate the magnetic field B_0 and chemical shift inhomogeneities and to measure the apparent T_2 relaxation time for mobile materials accurately.

Thus, both the SEPS and the HEPS experiments have to be used for an accurate study of rigid and soft domains in TPEs. The SEPS was used to determine the relaxation time and the fraction of the rigid domains. The HEPS was used to determine the relaxation time for the soft domains.

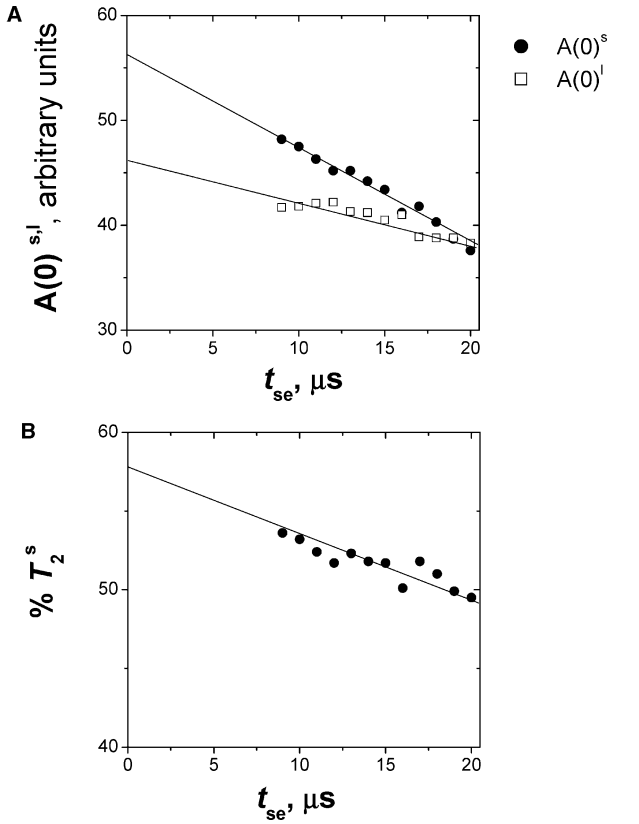

Figure 1. Initial amplitude of the fast (T_2^s relaxation) and slowly (T_2^l relaxation) decaying components (A) and the fraction of fast decaying component (B), as a function of t_{se} in the SEPS for the PBT homopolymer. The solid-echo experiment was performed at 130 °C.

The time constants (T_2), which are characteristic of different slopes in the magnetization decay curve, and the relative fraction of the relaxation components were obtained by performing a least-squares fit of the data using a linear combination of a Gaussian (rigid domains) and a stretched exponential (soft domains) function:

$$A(t) = A(0)^s \exp[-(t/T_2^s)^2] + A(0)^l \exp[-(t/T_2^l)^\alpha] \quad (1)$$

where the superscripts "s" and "l" correspond to short and long decay time, respectively. Since the parameter α in the stretched exponential function was about 0.8−0.9 for all samples, this suggests heterogeneous molecular mobility in the soft domains. It is noted that a quantitative analysis of the decay shape for soft materials is not always straightforward due to the complex origin of the relaxation function itself[24] and the structural heterogeneity of soft domains due to complex morphology of the TPEs. Therefore, T_2^l represents the apparent relaxation time of soft domains that are composed of a highly mobile PTMO phase and a less mobile PBT/PTMO mixed phase.[2,8] The relative fraction of the relaxation components—% $T_2^s = \{A(0)^s/[A(0)^s + A(0)^l]\} \times 100\%$ and % $T_2^l = \{A(0)^l/[A(0)^s + A(0)^l]\} \times 100\%$—is proportional to the hydrogen content in the rigid and soft domains that are discriminated in the present study on the basis of a distinct difference in the T_2 relaxation.

2. ^{1}H 2D DQ NMR BABA Experiments under Fast MAS. The general pulse sequence for multiple-quantum, two-dimensional experiments consisting of excitation, evolution, reconversion, and detection is shown in Figure 2a. Under fast MAS conditions employed here, the homonuclear dipolar coupling is strongly averaged out. Therefore, to reintroduce it, we employed the back-to-back sequence (BABA),[25] which is shown in Figure 2b. As a sequence block for excitation/

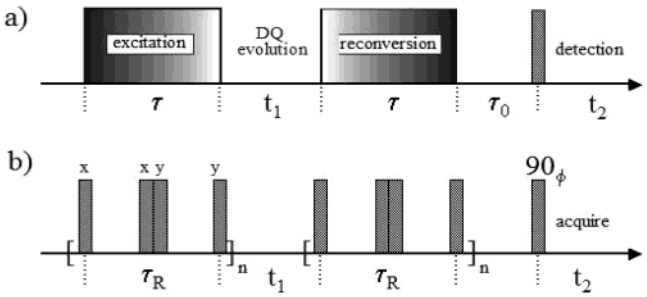

Figure 2. General scheme for excitation of DQ coherences with a *z*-filter (a) and rotor-synchronized BABA sequence, with *n* indicating the number of loops of BABA-cycles (b).

reconversion to reintroduce the dipolar interaction under MAS, four 90° pulses are placed within one full rotor period, τ_R, and two pulses with a 90° phase shift are placed back-to-back to each other at half the rotor period. Using a short excitation/reconversion period, a correlation peak between PBT and PTMO signals should indicate a close (through-space) connection between these blocks. For a detailed description of the pulse sequence the reader is referred to the literature.[25]

D. Proton NMR Transverse Magnetization Relaxation with Respect to Molecular Mobility and Phase/Components Composition. Proton T_2 relaxation experiments are often used for the analysis of microphase structure and molecular motions in polymer materials. The T_2 relaxation process is very sensitive to even small changes in molecular mobility, which can be seen from the range of T_2: from about 10 μs for glassy and crystalline materials to about a few seconds for low molar mass liquids. The large difference in T_2 shows that this experiment is highly sensitive to changes of composition and morphology in polymer materials, since these changes affect molecular mobility. A study of ^{1}H T_2 relaxation as a function of temperature provides information about molecular motions and phase transitions. Below the glass temperature (T_g), side groups and local chain motions cause a moderate change in T_2. The value of T_2 increases together with the amplitude and/or the frequency of molecular motions. The glass transition at the time scale of the NMR experiment, i.e., 10−100 μs, causes a sharp increase in T_2. It is noted that T_g, as measured by this NMR experiment, is comparable to the dynamic glass transition as measured by DMTA at a frequency of about 20−50 kHz and is usually observed at the temperature, which is 30−40 °C above T_g measured by DSC.

The NMR method can be used for a selective study of different components/(inter)phases in polymer materials, if the molecules/molecular fragments of those materials reveal a significant difference in molecular mobility. In this case, the T_2 relaxation function is a weighted sum of T_2 decays from different components/phases. The relative fraction of these components, % T_2, is proportional to the content of hydrogen in these (inter)phases/components. The characteristic decay time, T_2, is related to molecular mobility in different phases/components. The longer the T_2, the larger the frequency and/or amplitude of molecular motions is.

Results and Discussion

1. Rigid Fraction of TPEs and PBT Crystallinity. To find out the optimum temperature for determination of PBT crystallinity in TPEs, ^{1}H and ^{2}H NMR experiments on a PBT homopolymer are performed at different temperatures.

1.1. Molecular Mobility of PBT by ^{2}H NMR. The temperature dependence of the deuteron NMR spectrum for a selectively labeled PBT homopolymer with C_2D_4 fragments is shown in Figure 3.[19] The mobility of the deuterated chain fragments is frozen below 0 °C, as can be seen from the Pake-like shape of the spectrum. Upon increasing the temperature, the singularities disappear and a broad line appears in the middle part of the

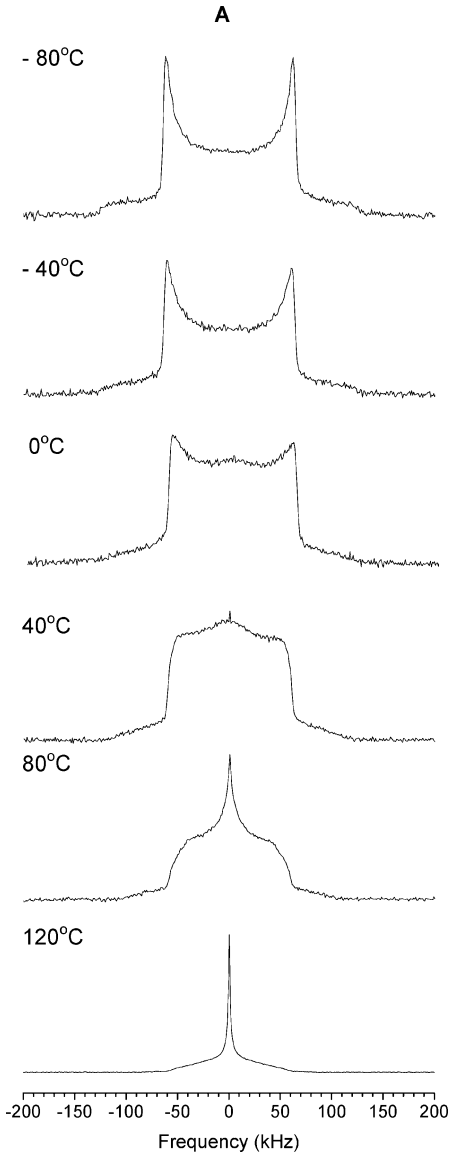

Figure 3. Temperature dependence of deuteron solid-echo spectra for the PBT homopolymer with selectively deuterated aliphatic fragments.[19]

spectrum. These spectral changes correspond to a gradual increase in the molecular mobility of the C_2D_4 fragments, which involve restricted reorientations of the ethylene fragments around 3−5 bonds of the main chain.[26] Above 80 °C, the spectrum is a superposition of broad and narrow lines, which is typical for semicrystalline polymers above T_g.[22] Since the T_g of the soft domains is observed at about −70 to −60 °C, NMR relaxation experiments in near room temperature should be highly selective to the relaxation of rigid and soft domains of PBT-*block*-PTMO. Similar conclusions follow from the ^{1}H T_2 relaxation data for the PBT homopolymer, which are discussed below.

1.2. Rigid Fraction of TPEs and PBT Crystallinity by ^{1}H T_2 Relaxation. Proton T_2 relaxation experiments are often used for the determination of crystallinity and phase composition in polymers.[12,27,28] In general, a good correlation is observed between crystallinity, as measured by NMR, compared to other methods.[12,29,30] However, a variety of methods on exactly the same sample do not always yield the same results[17,31] due to the following reasons: (a) complex morphology of semicrystalline polymers requiring different sets of

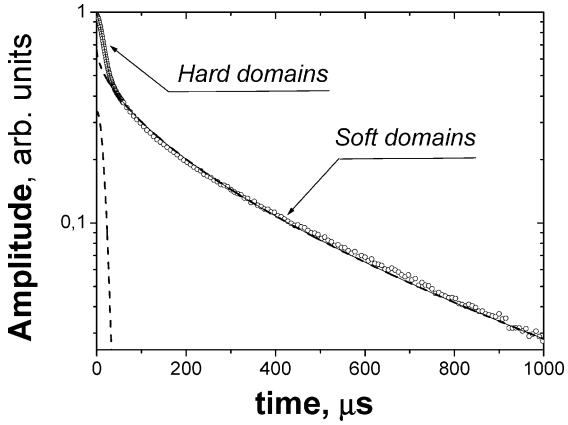

Figure 4. ^{1}H T_2 decay for sample A1000/35 at 40 °C, as measured with the SEPS. Open points show the experimental results. In addition to the overall least-squares adjusted decay (line), the individual fast (T_2^s relaxation) and slowly (T_2^l relaxation) decaying components are also shown by dashed lines.

assumptions for the analysis of data recorded by the different techniques; (b) the two-phase model is rather simplified for describing semicrystalline polymers due to the presence of a crystal−amorphous interface, which can be detected either as crystalline or amorphous fraction depending on the method used;[17,31] (c) discrimination of the crystalline phase from the amorphous one on a basis of different characteristics, such as the enthalpy of melting (DSC), long-range periodicity (WAXD), bond vibrations (vibrational spectroscopy), the specific volume (density analysis), and molecular mobility (NMR). Similar to other methods for crystallinity determination, crystallinity values, as determined by NMR, are also affected to some extent by the temperature of the experiment and a fitting function used for the deconvolution of FID into separate components.

The NMR measurements should be performed at temperatures well above T_g, yielding distinct differences in chain mobility in the crystalline and amorphous phases. To find the optimum temperature for determination of PBT crystallinity, we performed ^{1}H T_2 relaxation experiments as a function of temperature for PBT-*block*-PTMO (A1000/35 and A1000/60) and the PBT homopolymer. In the studied temperature range, the ^{1}H T_2 decay for all TPEs consists of two components that originate from the relaxation of rigid (T_2^s relaxation) and soft (T_2^l relaxation) domains (Figure 4). The PBT homopolymer also shows the two-component relaxation above 100 °C (Figure 5A). Above the dynamic glass transition temperature of PBT, the rigid fraction of PBT in the PBT homopolymer reaches a constant value of about 60% at 130 °C and starts to decrease when approaching the melting temperature, which is at about 230 °C.[18]

The effect of temperature on the content of the rigid fraction is compared for the PBT homopolymer and the TPEs with high and low soft block content in Figure 5B. The rigid fraction of PBT is significantly smaller in the TPEs compared to the PBT homopolymer (Figure 6), which is apparently caused by the short PBT block lengths in the case of TPEs. According to WAXD, only PBT blocks containing more than eight butylene terephthalate (BT) units can form crystallites.[7] Because of the molar mass distribution of PBT blocks ($M_w/M_n \approx 2$), PBT crystals in samples with shorter average block length are apparently formed by PBT blocks of the high

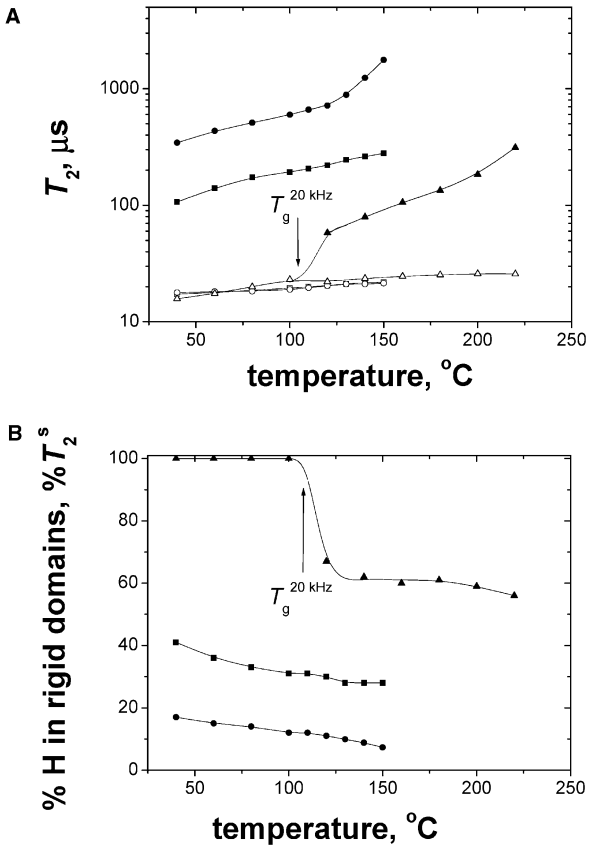

Figure 5. Temperature dependence of the T_2 relaxation time for the hard (open points, T_2^s relaxation) and the soft (filled points, T_2^l relaxation) fractions of the PBT homopolymer (triangles), sample A1000/35 (squares), and sample A1000/60 (spheres) (A) and the content of hydrogens in the rigid phase of these samples, % T_2^s (B). The arrow denotes the dynamic glass transition temperature for the PBT homopolymer at a frequency of about 20 kHz.

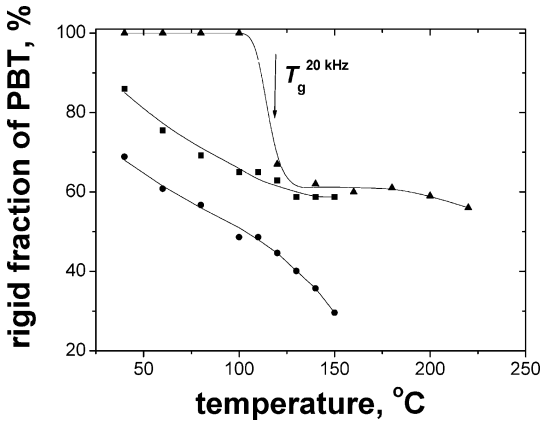

Figure 6. Temperature dependence of the rigid fraction of PBT in the PBT homopolymer (triangles) and in PBT blocks of sample A1000/35 (squares) and sample A1000/60 (circles). The rigid fraction of PBT, which consists of PBT crystals and immobilized chain portions at the crystal−amorphous PBT interface, is calculated from the sample composition. The arrow denotes the dynamic glass transition temperature for PBT at a frequency of about 20 kHz.

molar mass tail of the distribution.[7] The rigid fraction of PBT in the TPEs decreases with increasing temperature in a wide temperature range and approaches zero at the melting temperature, as it can be seen for A1000/60 for which $T_m \approx 157$ °C.[18] This gradual decrease in the content of the rigid phase is caused by a wide range

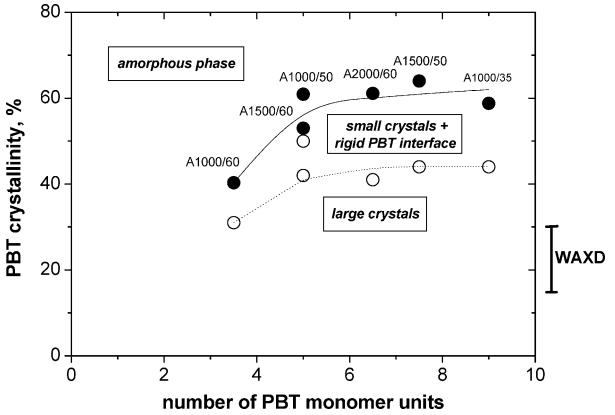

Figure 7. Crystallinity of the PBT blocks in TPEs series A as a function of the number-average length of the PBT blocks. The crystallinity was determined by DSC (open circles)[18] and by NMR (filled circles) at 130 °C. It is noted that annealing of samples during NMR experiments can cause the difference in crystallinity.[33] The range of WAXD crystallinity of as-prepared samples is shown of the right side of the *y*-axis.[7]

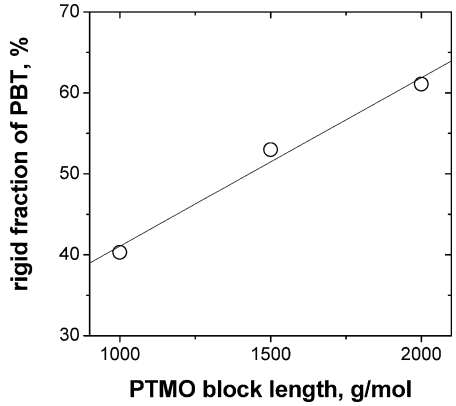

Figure 8. NMR crystallinity of PBT in TPE series A as a function of the length of the PTMO block. The PTMO content in all samples is 60 wt %. The crystallinity was measured at 130 °C.

of melting temperatures of the PBT crystals due to a distribution in crystal size and crystal perfections, also visible in a broad melting peak in DSC experiments.[7]

The rigid fraction of PBT, which is calculated from % T_2^s for the TPEs-A series, is compared for all samples at 130 °C (Figure 7). This temperature is chosen because of the following reasons. (1) This temperature is significantly lower than the melting temperature of the PBT homopolymer. (2) The content of low mobile PBT chains in the PBT homopolymer is nearly constant above this temperature (Figure 5B). Therefore, % T_2^s at 130 °C is less affected by a change in the content of the semirigid crystal−amorphous PBT interface above this temperature, which allows us to estimate the crystallinity by this NMR method. (3) The chain mobility in rigid and soft domains differs significantly at this temperature, as is can be concluded from the distinct differences in T_2^s and T_2^l, which results in a more reliable least-squares fit of the FIDs. Thus, the rigid fraction of the PBT at 130 °C represents the crystallinity at this temperature, as measured by NMR. The NMR crystallinity includes nanocrystals and crystals with a large fraction of defects[17,27,28] as well as immobilized PBT chain portions at the crystal−amorphous PBT interface—partially ordered material adjacent to the crystal surface.

The NMR crystallinity of PBT homopolymer is about 1.5 times larger than its value for a typical PBT sample measured by DSC experiments (about 44%) (Figure 7).[18] The NMR crystallinity of PBT in TPEs is also larger compared to the crystallinity as determined by WAXD.[7] This difference between DSC, WAXD, and NMR methods can be explained by the different origin of the methods and assumptions made for data analysis, as discussed above. The crystallinity, as determined by DSC, can be underestimated due to the presence of small and imperfect crystals whose heat of melting is smaller compared to large and "perfect" crystals. WAXD determines only large crystals consisting of several crystal unit cells,[32] whereas NMR allows measuring nanosize crystals.[17,27,28] The larger NMR crystallinity, as compared to its value from WAXD, suggests that a large number of smaller crystals are formed in TPEs. Annealing of the samples during the NMR experiment can also cause some increase in the NMR crystallinity, as compared to the DSC and WAXD data.[33] Therefore, DSC, WAXD, and NMR experiments for samples with the same thermal history are required for better understanding of the effect of annealing on PBT crystallinity.

The crystallinity of PBT blocks in PBT-*block*-PTMO is plotted against the length of the PTMO block in Figure 8. The PBT crystallinity increases with increasing length of the soft block for the samples with the same PTMO content, since this results in an increase in the average length of PBT blocks. The NMR and DSC crystallinity is nearly constant for TPEs with the average length of the PBT block above five butylene terephthalate (BT) units. It is in contrast to results of WAXD study that suggests that PBT blocks containing less than eight BT units cannot form crystallites.[7] Thus, the NMR data suggest that short PBT blocks can form disordered crystals and defects in larger crystals that are detected by WAXD experiments as the amorphous fraction.[27]

2. Phase Composition of TPE's. 2.1. Miscibility of Soft and Hard Blocks As Studied by ^{1}H 2D DQ NMR BABA Experiments. Previous ^{13}C NMR MAS relaxation experiments revealed a large, bimodal-like heterogeneity of the PTMO chain mobility, which was explained by microphase separation of the amorphous phase into a highly mobile PTMO-rich phase and a less mobile PBT/PTMO mixed phase (PBT/PTMO interface).[2,8] However, the motional heterogeneity of the PTMO blocks can also originate from a dynamical interface due to anchoring of PTMO blocks to rigid PBT domains, which can cause apparent "two-phase" behavior.[9,10] 2D NMR experiments can provide direct information on the molecular scale miscibility in polymeric materials.[11] ^{1}H-DQ correlation spectroscopy under fast-MAS using the back-to-back (BABA) sequence is used in the present study to determine the proximity of the PBT and PTMO chain units in the block copolymers.

The ^{1}H MAS NMR spectrum of PBT-*block*-PTMO consists of resonances at 8.0, 4.4, 3.4, and 1.6 ppm that originate from the aromatic protons of PBT, the OCH_2 protons of PBT, the OCH_2 protons of PTMO, and the $(CH_2)_2$ protons of PBT and PTMO, respectively. It is noted that the OCH_2 protons of PBT and PTMO at the transition from PBT to PTMO blocks along the chain have slightly different chemical shifts, as measured by ^{1}H solution NMR spectra, i.e., 4.35 and 3.45 ppm for PBT and PTMO, respectively. However, these resonances are not resolved in the solid-state NMR spectra.

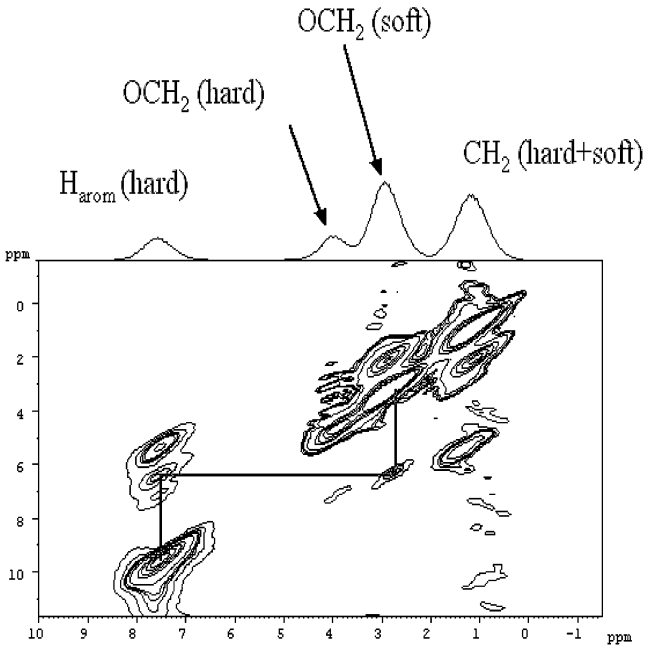

Figure 9. 2D ^{1}H BABA spectrum for sample A1000/35 showing the correlations between the resonances of PBT and PTMO chain units, as indicated by the lines connecting the peak positions.

Figure 9 shows the phase-sensitive 2D spectrum of sample A1000/35 measured using the BABA sequence with two rotor periods of excitation/reconversion recorded using the TPPI method.[34] The single quantum (SQ) and double quantum (DQ) dimensions are shown on the horizontal and vertical axes, respectively. The signals in the DQ dimension are situated at the sum of the frequencies of the two coupled protons. Therefore, a DQ signal between two protons with identical chemical shifts will be on the diagonal, and signals between two protons with different chemical shifts will be off-diagonal, giving rise to two signals equally spaced from the diagonal. One should note the different positions of off-diagonal signals are compared to COSY/NOESY spectra.

As expected, all resonances of PBT and PTMO blocks are present in the 2D spectrum, i.e., all diagonal peaks and off-diagonal correlation peaks between the aromatic and the OCH_2 protons of PBT as well as a correlation peak between the CH_2 and OCH_2 peaks of PTMO. Additionally, there is a correlation peak between the aromatic protons from PBT and the OCH_2 groups from PTMO, suggesting a close proximity of these two chain fragments. The signal is in fact much more intense than one would expect (i) from a small fraction (only 14%) of PTMO chain units that are located at the transition from PBT to PTMO blocks in a single chain and (ii) from the rather long intrachain distance between aromatic PBT and the OCH_2 protons of PTMO at the transition from the hard to the soft blocks along the chain. The correlation peak cannot be explained by spin diffusion during the 1 ms *z*-magnetization delay after the reconversion period.[35] Therefore, the DQ BABA MAS experiment is not affected essentially by the spin diffusion process and gives information about the molecular scale mixing. This correlation peak has to come primarily from intermolecular couplings between the PBT and PTMO protons of adjacent chains. In fact, it was shown that a DQ correlation signal arises at short recoupling times, which in our case, marks an interproton distance below 0.5 nm.[36] Therefore, this correlation peak can be unambiguously attributed to PBT and PTMO units in a mixed PBT/PTMO phase.

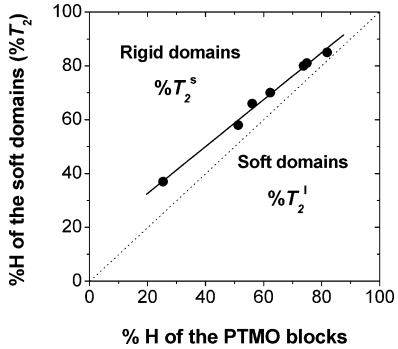

Figure 10. Fraction of hydrogens in the soft domains (% T_2^l), as determined by NMR at 40 °C, against the hydrogen fraction (% H) in the PTMO blocks according to the sample composition of TPEs series A. The dotted line with slope 1 is a guide to the eye. The solid line represents the result of a linear regression analysis: intercept = 15 ± 2% T_2^l; slope = 0.87 ± 0.03 % T_2^l/% H. The correlation coefficient is 0.997.

HARD DOMAINS		SOFT DOMAINS	
T_2^s relaxation		T_2^l relaxation	
Crystalline PBT	Rigid crystal-amorphous PBT interface	PBT/PTMO mixed phase Composed of 30±5 wt. % PBT and 70±5 wt. % PTMO	PTMO-rich phase

Figure 11. Schematic drawing of the microphase composition of PBT-*block*-PTMO according to ^{1}H and ^{13}C NMR data.

2.2. Phase Composition and the PBT/PTMO Interface Investigated by ^{1}H and ^{13}C NMR Relaxation Experiments. To determine the phase diagram of PBT-*block*-PTMO, results of ^{1}H and ^{13}C NMR relaxation experiments are used. ^{1}H T_2 relaxation data are used to determine the fraction of rigid and soft domains. ^{13}C NMR experiments, which were performed previously,[2,8] provide quantitative data on the content of the PTMO-rich phase. The phase composition in the TPEs-A series was determined at 40 °C, since this temperature is below the T_g for the PBT homopolymer (Figure 5B).

The relative intensity of relaxation components (% T_2^s and % T_2^l) is compared in Figure 10 to the calculated hydrogen fraction of PTMO. The fraction of hydrogen in soft domains is larger compared to that in the soft blocks. Since the experiments are performed at 40 °C, which is below T_g for the PBT homopolymer, this means that some of the PBT chain units reveal fast chain mobility. This mobile fraction of PBT is apparently mixed with the soft PTMO blocks and contributes to the T_2^l relaxation of the soft domains. The microphase structure of TPE's, which follows from this simplified model, is shown in Figure 11.

From the results of the present and previous ^{13}C NMR studies,[2,8] the phase diagram of PBT-*block*-PTMO can be determined (Figure 12). The fraction of rigid and mixed PBT is calculated from % T_2^s, the sample composition, and hydrogen content in PBT and PTMO. The fraction of mixed PTMO and PTMO-rich phase was determined in previous ^{13}C NMR experiments.[2,8] The fraction of the PBT/PTMO mixed phase and the absolute amount of mixed PBT and PTMO are nearly identical for all samples (see Figures 12 and 13). About 35 wt % of all samples resides in the mixed phase. The mixed

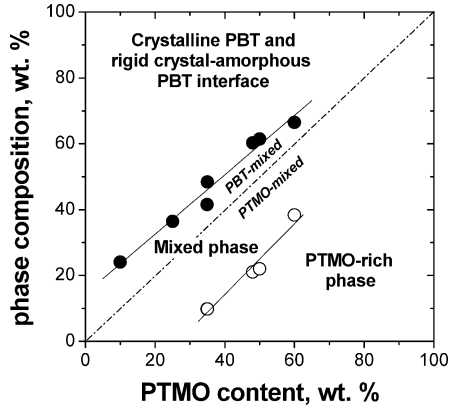

Figure 12. Phase composition of TPEs series A at 40 °C against the content of PTMO block (in wt %). The dash−dotted line of slope 1 is a guide to the eye. The straight lines represent the result of a linear regression analysis for the fraction of PTMO-rich phase (intercept = −29 ± 5 wt %; slope = 1.1 ± 0.1; the correlation coefficient equals 0.981) and for PBT rigid domains (intercept = 15 ± 3 wt %; slope = 0.90 ± 0.07; the correlation coefficient is 0.986).

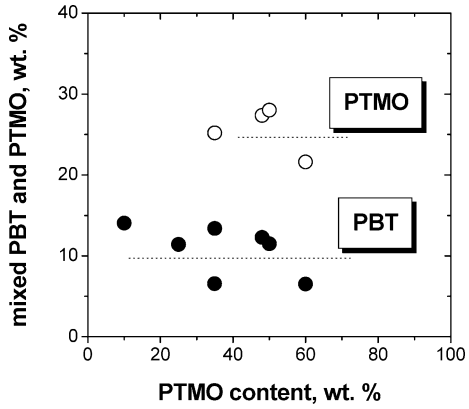

Figure 13. Amount of mixed PBT and PTMO (in wt % of the total weight) against the PTMO content in TPEs series A.

phase is composed of 35 ± 5 wt % PBT and 65 ± 5 wt % PTMO, which is about one PBT chain unit per about eight PTMO chain units. The nearly constant composition of the mixed phase in all samples with a large variety of composition and PBT and PTMO block length suggests the thermodynamic origin of the mixing and not a dynamic interface due to anchoring of soft blocks at rigid PBT domains. The increase in the soft block content causes a decrease in the rigid (crystalline) fraction of PBT and an increase in the content of the PTMO-rich phase, as can be seen in Figure 12. Thus, the contents of soft and hard blocks as well as the block length largely affect the microphase composition of PBT-*block*-PTMO.

3. Effect of Miscibility on the Chain Mobility in Soft Domains. In addition to the phase composition, the NMR T_2 relaxation method provides information on the chain mobility in the soft domains. Knowledge of the chain mobility in the soft domains is of great importance for an understanding of the viscoelastic properties of TPEs. Our previous studies on rubbers and rubber phases have shown that the information obtained by NMR is closely related to the viscoelasticity and some other mechanical properties.[37−39] The temperature dependence of the T_2 relaxation time for the soft and hard domains of two TPEs of series A is shown in Figure 5A. The content of soft domains increases with increasing temperature, which results in a change in the composition of the soft domains due to a gradual melting of PBT crystals (see Figure 5B).

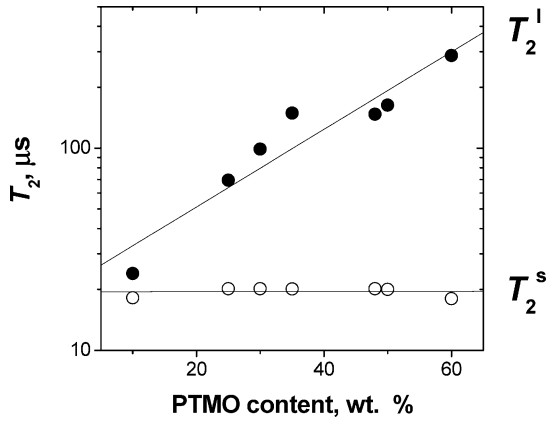

Figure 14. ^{1}H T_2^s and T_2^l relaxation time at 40 °C for the hard and soft domains against the PTMO content for TPE series B. The length of the PTMO blocks in all samples is 1000 g/mol.

A comparison of the T_2^l relaxation time for the TPE-B series, which contains different amounts of PTMO blocks with the same block length, reveals the following changes in chain mobility in the soft domains (Figure 14). The chain mobility in the soft domains increases substantially with increasing PTMO content from 10 to 60 wt %, which follows from an approximately 10-fold increase of T_2^l. In contrast, the mobility in the hard domains is not affected by the content of the PTMO blocks. Since the molar mass of the soft block is the same in all these samples (1000 g/mol), the chain-anchoring effect, i.e., immobilization of PTMO chain units adjacent to the PBT block, should be the same for all samples. Therefore, the chain anchoring is not the main reason for restriction of the chain mobility in the soft domains upon increasing amount of PBT. The following other factors can hinder chain mobility in the soft domains of TPEs upon increasing PBT content: (1) enrichment of the soft domains with a less mobile PBT/PTMO mixed phase (see Figure 12); (2) an increase in the density of topological knots (entanglements) between the hard and soft domains due to a larger interfacial area between hard and soft domains per unit volume of the soft domains; (3) an increase of chain confinement in the soft domains by the rigid domains, which impose entropy constraints and therefore hinder large-amplitude chain mobility. Apparently, the mobility of a single PTMO block in TPEs with the smallest soft block content is hindered by a few physical/topological constraints from the hard domains, since T_2^l decreases by about 10 times with the decrease of the PTMO block content from 60 to 10 wt %. It can be suggested that nonequilibrium viscoelastic properties of the TPEs might be affected by physical/topological hindrances on chain mobility of PTMO blocks. A more detailed analysis of chain mobility in the soft domains is provided in the follow-up paper of this study.[40]

Conclusions

^{1}H and ^{13}C solid-state NMR experiments provide strong evidence of partial thermodynamic mixing of PBT and PTMO blocks in PBT-*block*-PTMO-based TPEs. The ^{1}H 2D DQ BABA experiment shows a close proximity of the aromatic protons from PBT and PTMO OCH_2 protons, suggesting molecular scale mixing of PBT and PTMO blocks. Three different nano(micro)phases coexist

at 40 °C in the TPE's, i.e., a crystalline PBT, a PBT/PTMO mixed phase, and a PTMO-rich phase. The chemical composition of the mixed phase is not affected by the content and the length of the PTMO blocks. At 40 °C, the mixed phase is formed by about one PBT chain unit per about eight PTMO chain units. Rigid domains are formed by crystalline PBT and immobilized PBT chain portions at the crystal−amorphous PBT interface, whereas soft domains are composed of PBT/PTMO mixed phase and PTMO-rich phase. The NMR T_2 relaxation experiments allow determination of the phase diagram of this TPE as well as of the crystallinity of PBT. The content and the length of the soft blocks largely affect the phase composition and molecular mobility in the soft domains. It is suggested that this information is of interest for a better understanding of the hardness and the viscoelastic properties of the TPEs.

Acknowledgment. The authors are grateful to R. Scherrenberg and T. Pijpers for providing the results of the DSC experiments and W. Gabriëlse for recording ^{2}H NMR spectra of a selectively deuterated PBT homopolymer. The authors appreciate A. Schmidt's comments on the manuscript.

References and Notes

(1) Adams, R. K.; Hoeschele, G. K.; Witsiepe, W. K. *Thermoplastic Elastomers*, 2nd ed.; Holden, G., Legge, N. R., Quirk, R., Schroeder, H. E., Eds.; Hanser Publishers: Munich, 1996.
(2) Gabriëlse, W.; Soliman, M.; Dijkstra, K. *Macromolecules* **2001**, *34*, 1685 and references therein.
(3) Miller, J. A.; McKenna, J. M.; Pruckmayr, G.; Epperson, J. E.; Cooper, S. L. *Macromolecules* **1985**, *18*, 1727.
(4) Soliman, M.; Dijkstra, K.; Borggreve, R. J. M.; Wedler, W.; Winter, H. H. *Makromolekulares Kolloqium*; Freiburg, 1998.
(5) Veenstra, H.; Hoogvliet, R. M.; Norder, B.; Postuma de Boer, A. *J. Polym. Sci., Part B* **1998**, *36*, 1796.
(6) Wegner, G.; Fujii, T.; Meyer, W.; Lieser, G. *Angew. Makromol. Chem.* **1978**, *74*, 295.
(7) Konyukhova, E. V.; Neverov, V. M.; Godovsky, Y. K.; Chvalun, S. N.; Soliman, M. *Macromol. Mater. Eng.* **2002**, *287*, 250.
(8) Schmidt, A.; Veeman, W. S.; Litvinov, V. M.; Gabriëlse, W. *Macromolecules* **1998**, *31*, 1652.
(9) Resing, H. A. *J. Chem. Phys.* **1965**, *43*, 669.
(10) Rössler, E.; Taupitz, M.; Börner, K.; Schulz, M.; Vieth, H.-M. *J. Chem. Phys.* **1990**, *92*, 5847.
(11) Schmidt-Rohr, K.; Spiess, H. W. *Multidimensional Solid-State NMR and Polymers*; Academic Press: London, 1994.
(12) McBrierty, V. J.; Packer, K. J. *Nuclear Magnetic Resonance in Solid Polymers*; Cambridge University Press: Cambridge, 1993.
(13) Stöppelman, G.; Gronski, W.; Blume, A. *Polymer* **1990**, *31*, 1838.
(14) Litvinov, V. M.; Barthel, H.; Weis, J. *Macromolecules* **2002**, *35*, 4356.
(15) Wouters, M. E. L.; Litvinov, V. M.; Binsbergen, F. L.; Goossens, J. G. P.; van Duin, M.; Dikland, H. G. *Macromolecules* **2003**, *36*, 1147.
(16) Litvinov, V. M. In *Spectroscopy of Rubbers and Rubbery Materials*; Litvinov, V. M., De, P. P., Eds.; Rapra Technology Ltd.: Shawbury, 2002; p 353.
(17) Litvinov, V. M.; Mathot, V. B. F. *Solid State Nucl. Magn. Reson.* **2002**, *22*, 218.
(18) Scherrenberg, R.; Pijpers, T. Unpublished results.
(19) Gabriëlse, W.; van Guldener, V.; Schmatz, H.; Abetz, V.; Lange, R. *Macromolecules* **2002**, *35*, 6946.
(20) Bilski, P.; Sergeev, N. A.; Wasicki, J. *Mol. Phys. Rep.* **2000**, *29*, 55.
(21) Kimmich, R. *NMR−Tomography, Diffusiometry, Relaxometry*; Springer-Verlag: Berlin, 1997.
(22) Spiess, H. W. *Colloid Polym. Sci.* **1983**, *261*, 193.
(23) Bilski, P.; Segreev, N. A.; Wasicki, J. *Mol. Phys.* **2003**, *101*, 335.
(24) Cohen-Addad, J. P. *Prog. NMR Spectrosc.* **1993**, *25*, 1 and references therein.
(25) Feike, M.; Demco, D. E.; Graf, R.; Gottwald, J.; Hafner, S.; Spiess, H. W. *J. Magn. Reson. A* **1996**, *122*, 214.
(26) Hentschel, D.; Sillescu, H.; Spiess, H. W. *Polymer* **1984**, *25*, 1078.
(27) Barendswaard, W.; Litvinov, V. M.; Souren, F.; Scherrenberg, R. L.; Gondard, C.; Colemonts, C. *Macromolecules* **1999**, *32*, 167.
(28) Litvinov, V. M. *Macromolecules* **2001**, *34*, 8468.
(29) Hansen, E. W.; Kristiansen, P. E.; Pedersen, B. *J. Phys. Chem. B* **1998**, *102*, 5444. Kristiansen, P. E.; Hansen, E. W.; Pedersen, B. *J. Phys. Chem. B* **1999**, *103*, 3552.
(30) Eckman, R. R.; Henrichs, P. M.; Peacock, A. J. *Macromolecules* **1997**, *30*, 2474.
(31) Isasi, J. R.; Mandelkern, L.; Galante, M. J.; Alamo, R. G. *J. Polym. Sci., Polym. Phys. Ed.* **1999**, *37*, 323.
(32) The dimensions of the unit cell of the α-crystalline phase of PBT are the following: 0.483 nm (*a*), 5.94 nm (*b*), and 11.59 nm (*c*) (see: Miller, R. L. In *Polymer Handbook*, 4th ed.; Brandrup, J., Immergut, E. H., Grulke, E. A., Eds.; John Wiley & Sons: New York, 1999; p VI/48).
(33) The NMR experiment at 130 °C takes a significantly longer time compared to sample exposure to elevated temperatures in DSC experiments. The WAXD experiment was performed at room temperature. The NMR experiment for TPE A1500/50 shows that annealing of the sample at 180 °C for 40 h causes about 25% increase in the NMR crystallinity. Therefore, the difference between PBT crystallinity, as measured by DSC, WAXD, and NMR methods, cannot be explained only by the difference in the thermal history of the samples.
(34) Drobny, G.; Pines, A.; Sinton, S.; Weitekamp, D. P.; Wemmer, D. *Faraday Symp. Chem. Soc.* **1978**, *13*, 49.
(35) To estimate the average distance of the magnetization transfer by spin diffusion, we assume an average value of spin diffusion coefficients of rigid and mobile regions of about $D = 2 \times 10^{-16}$ m^2 s^{-1}. The average distance can be evaluated using the relationship $(\Delta z^2)^{1/2} \cong (2Dt_{sd})^{1/2}$. For a filter time of the DQ experiments $t_f = t_{sd}$ of about 1 ms, during which the spin diffusion process is active the average distance is 0.6 nm.
(36) Schnell, I.; Spiess, H. W. *J. Magn. Reson.* **2001**, *151*, 153.
(37) Litvinov, V.; Steeman, P. A. M. *Macromolecules* **1999**, *32*, 8476.
(38) Steenbrink, A. C.; Litvinov, V. M.; Gaymans, R. J. *Polymer* **1998**, *20*, 4817.
(39) Litvinov, V. M.; Dias, A. A. *Macromolecules* **2001**, *34*, 4051.
(40) Bertmer, M.; Gasper, L.; Demco, D. E.; Blümich, B.; Litvinov, V. M. *Macromol. Chem. Phys.*, in press.

MA030314H